Journal of Power Sources 195 (2010) 3785–3793

Contents lists available at ScienceDirect

Journal of Power Sources

journal homepage: www.elsevier.com/locate/jpowsour

Anion-exchange membranes composed of quaternized-chitosan derivatives for alkaline fuel cells

Ying Wan[a,b], Brant Peppley[b,c,*], Katherine A.M. Creber[a], V. Tam Bui[a]

[a] Department of Chemistry and Chemical Engineering, Royal Military College of Canada, Kingston, Ontario, Canada K7K 7B4
[b] Queen's Royal Military College Fuel Cell Research Centre, Kingston, Ontario, Canada K7L 5L9
[c] Department of Chemical Engineering, Queen's University, Kingston, Ontario, Canada K7L 3N6

ARTICLE INFO

Article history:
Received 2 October 2009
Received in revised form
21 November 2009
Accepted 25 November 2009
Available online 1 December 2009

Keywords:
Quaternized-chitosan
Anion-exchange membrane
Alkaline fuel cell

ABSTRACT

A series of quaternized-chitosan derivatives (QCDs) with various degrees of quaternization was synthesized using glycidyltrimethylammonium chloride as a main quaternized reagent. These QCDs were then processed into hydroxide—form quaternary ammonium salts with aqueous potassium hydroxide solutions. The resultant hydroxide—form QCD gels were further crosslinked into anion-exchange membranes using ethylene glycol diglycidyl ether. The crosslinking density, crystallinity, swelling index, ion exchange capacity, ionic conductivity and thermal stability of the crosslinked membranes were subsequently investigated. It was found that properties of crosslinked membranes were modulated mainly by the degree of quaternization and crosslinking density of membranes. Some membranes exhibited promising characteristics and had the potential for applications in alkaline polymer electrolyte fuel cells in considering their integrative properties.

1. Introduction

Polymer electrolyte fuel cells (PEFCs) have received great attention for years due to their clean and highly efficient characteristics. Among different types of PEFCs, the direct methanol fuel cells (DMFCs) have been increasingly believed to be a promising candidate commercially available for portable power devices because of the ease use and storage of methanol [1]. It is known that DMFCs currently utilize proton exchange membranes as main carriers of cations. Of these proton exchange membranes, perfluorinated membranes, commercially known as Nafion membranes, have been preferentially used for DMFCs. Despite the wide usability of Nafion membranes, several disadvantages, such as slow anode kinetics, parasitic methanol crossover and the requirement for expensive platinum-based catalysts, have obstructed the commercialization of DMFCs [2]. Many efforts, therefore, have been directed towards developing new types of polymer electrolyte membranes for DMFCs. Besides unceasingly exploring new types of proton exchange membranes, anion-exchange membranes have also aroused new interest in recent years. It has been suggested that if alkaline polyelectrolyte membranes are employed for DMFCs, then several potential benefits can be expected [3–8]: (a) facile kinetics at the cathode as well as at the anode; (b) more effective oxidation of methanol in the alkaline media; (c) reduced level of methanol crossover from anode to cathode; (d) available non-noble metal catalysts (such as nickel and silver), and (e) cheaper, more easily machined metal bipolar plates, and minimizing electrode weeping and component corrosion.

Chitosan, a derivative of chitin, is a low-cost biopolymer and a weak alkaline polyelectrolyte [9]. In the dry state, a crosslinked unmodified-chitosan membrane is almost non-conductive. However, after being fully hydrated, a hydrated chitosan membrane shows an ionic-conductive characteristic [10]. Nevertheless, our previous results revealed that although an open circuit voltage of around 1.0 V could be reached by directly applying this type of membranes to an alkaline fuel cell, a low current density would be obtained [11], suggesting that conductivity of membranes was not high enough for applications in practical fuel cells, and ionic migration rate through the membranes may also need increasing.

Several techniques have been employed to produce various anion-exchange membranes [11,12–17]. Chitosan derivatives with side chains containing quaternary ammonium groups can function as positive-charge-rich gels and have been used as antimicrobial or antibacterial reagents [18,19] even though these derivatives have the potential for producing anion-exchange membranes. Some attempts have also been made to develop anion-exchange composite membranes by incorporating quaternized-chitosan into poly(vinyl alcohol) [20]. However, very little has been done to use pure quaternized-chitosan membranes for alkaline fuel cells. Considering that crosslinked quaternized-chitosan membranes with a relatively high degree of quaternization (DQ) could serve as

* Corresponding author at: Queen's Royal Military College Fuel Cell Research Centre, Kingston, Ontario, Canada K7L 5L9.
E-mail address: brant.peppley@queensu.ca (B. Peppley).

0378-7753/$ – see front matter © 2009 Elsevier B.V. All rights reserved.
doi:10.1016/j.jpowsour.2009.11.123

an anion exchange carrier for alkaline fuel cells, we have prepared some crosslinked membranes using glutaraldehyde (GA) as crosslinker and applied this type of membranes to a real alkaline fuel cell system, achieving a current density of around 70 mA cm^{-2} at 50 °C by using hydrogen as fuel (50 mL min^{-1}) and air as oxidant (250 mL min^{-1}) [21]. However, it is found that GA is not effective enough for crosslinking quaternized-chitosan membranes with a higher DQ (for example, DQ > 35%) because the resultant quaternized-chitosan membranes crosslinked by GA frequently show a poor mechanical characteristic. It is therefore quite necessary to seek for a new type of crosslinker for crosslinking quaternized-chitosan membranes. In the present work, a desirable crosslinker, ethylene glycol diglycidyl ether, was introduced to prepare crosslinked quaternized-chitosan membranes with the aid of a newly developed processing technique. Some results about the preparation and characterization of crosslinked quaternized-chitosan membranes and relevant investigations into their chemicophysical properties were reported.

2. Experimental

2.1. Materials

Chitosan was purchased from Aldrich. To obtain highly deacetylated chitosan, the purchased chitosan samples were treated in a 50 wt.% NaOH solution at 100 °C for 2 h, and the alkali treatment was repeated one more time. The filtered products were washed with deionized water until a neutral pH was reached. Degree of deacetylation and viscosity average molecular weight of chitosan samples were measured as 96.8(±2.4)% and 2.37(±0.17) × 10^5, respectively, according to our previous methods [22]. Molecularporous membrane tubing used for dialysis was supplied by Fisher. All deuterated chemicals were provided by CDN ISOTOPES Inc., and other chemicals were all obtained from Aldrich and used as received.

2.2. Synthesis of HTCC and preparation of crosslinked quaternized-chitosan membranes

N-[(2-Hydroxy-3-trimethylammonium)propyl] chitosan chloride (referred to HTCC) was synthesized following a method similar to those described elsewhere [23,24]. To change HTCC into *N*-[(2-hydroxy-3-trimethylammonium)propyl] chitosan hydroxide (designated as HTCH), the obtained HTCCs with various DQs were added into different flasks containing a freshly prepared 1.0 M KOH solution, and mixtures were stirred at room temperature for 36 h. Each filtered product, HTCH, was sealed in a dialysis tube and dialyzed in running water until pH inside the tube reached about 8 while HTCH became a highly swollen gel. A given amount of HTCH gel was diluted into a concentrated solution with deionized water, and to this solution, a prescribed amount of ethylene glycol diglycidyl ether (EGDE) in ethanol was introduced. The mixture was stirred at 60 °C for 1 h and cast into a membrane on a specially constructed Plexiglas dish designed for fitting into the fuel cell test assembly. The dish was placed in an oven and solvent was allowed to be slowly evaporated while the membrane was progressively crosslinked at 60 °C for 12 h. Finally, the crosslinked HTCH membranes were thoroughly washed with deionized water, dried in air for two days and in vacuum at 80 °C for additional 12 h.

Two different sets of HTCH membranes were prepared. One set was coded as HTCH-*i* (*i* = *a*, . . ., *f*) and the membranes in this set were crosslinked with various amounts of crosslinker but DQ was maintained as a constant; another set was named as HTCH-*j* (*j* = 1, . . ., 6) and the resultant membranes in this group were crosslinked with the same amount of crosslinker but DQ was changed in a selected range. Some uncrosslinked HTCH membranes were also prepared by dissolving HTCH gels into deionized water to produce different solutions and the resultant solutions without any crosslinker were cast onto Plexiglas dishes. Thus produced uncrosslinked HTCH membranes were dried both in air and in vacuum, and used as controls. The uncrosslinked membranes were designated as UN-HTCH (*k*), where *k* denotes the DQ of HTCH in percentage. In addition, an uncrosslinked chitosan membrane was produced via a common method [22] and used as another control.

2.3. Characterization

IR spectra of HTCC were recorded on a Nicolet 510P FTIR spectrometer in transmission mode with 32 scans and a resolution of 2 cm^{-1}. All samples were prepared as KBr pellets and were scanned against a blank KBr pellet background.

HTCC powder was dissolved in 0.1–0.3% (v/v) CD_3COOD/D_2O and the obtained solutions were introduced into different 5-mm NMR tubes. ^{1}H NMR measurements were performed on a Bruker Advance 500 spectrometer using sodium 4,4-dimethyl-4-silapentanoate-2,2,3,3-d_4 as the internal reference.

DQ of HTCC was determined with two different methods. HTCC samples were dissolved in a 0.1 M HAc solution and the resultant solutions were titrated with an aqueous $AgNO_3$ solution to measure the amount of Cl^- ions which is proportional to the DQ of HTCC (24). The content of C, H, and N in HTCC was also determined using a Vario EL III elemental analysis instrument and DQ was calculated using the results of elemental analysis.

The crosslinking density (ρ) of HTCH membranes, which is inversely related to the average molecular weight per crosslinking unit and is also indirectly linked to the degree of crosslinking, was estimated from the network theory of rubber elasticity using the following equation [25]:

$$\rho = \frac{E'}{3d\phi RT} \quad (1)$$

where storage modulus, E', was determined using a dynamic mechanical analyzer (DMA Q800, TA Instruments) at a frequency of 1 Hz and a temperature of 40 °C; d, membrane density measured by using mixed solvents composed of carbon tetrachloride (density: 1.586 g cm^{-3}) and ethanol (density: 0.816 g cm^{-3}) via a floating method; ϕ, the front factor (where ϕ = 1); R, the gas constant; and T, the absolute temperature.

In respect to the measurement of ion exchange capacity (IEC), a piece of precisely weighed HTCH membrane was immersed in a 0.1 M HCl standard solution (20 mL) at ambient temperature for 24 h with occasional stirring, and then the solution containing the membrane was titrated back to neutralization with a 0.1 M KOH standard solution. End-points were determined from the maximum points registered in the differential titration plots. Three replicates were conducted for each sample and a blank run (without membrane) was also performed. IEC was calculated as follows:

$$\mathrm{IEC} = \frac{[N_{\mathrm{HCl},i} - N_{\mathrm{HCl},f}]}{M_{\mathrm{dry}}} \quad (2)$$

where $N_{\mathrm{HCl},i}$ is the HCl quantity (equivalent) in the initial solution (0.1 M, 20 mL), $N_{\mathrm{HCl},f}$, the remaining amount of HCl (equivalent) determined by the titration, and M_{dry}, the mass of dry membrane samples.

Thermogravimetric (TG) analysis was performed on a TGA 2050 analyzer (TA Instruments). Samples (ca. 10 mg) were heated from 30 to 400 °C at a heating rate of 10 °C min^{-1} under a nitrogen atmosphere.

X-ray diffractograms were recorded at room temperature with a X-ray diffractometer (SCINTAG X1). Dry membranes were mounted on aluminum frames and scanned from 5° to 40° (2θ) at a speed of 2° min^{-1}. To measure the relative crystallinity percentage (X_c)

of membranes, the amorphous areas and the areas of crystalline peaks were measured, respectively, and X_c was calculated with the following relationship [10]:

$$X_c\,\% = \left[\frac{A_c}{(A_c + A_a)}\right] \times 100\% \quad (3)$$

where A_c and A_a are the areas of crystalline peaks and amorphous section, respectively.

Water uptake of HTCH membranes was estimated by measuring the swelling index (SI) of membranes. Dry membrane (mass = W_d) was immersed in an excess amount of deionized water at ambient temperature until swelling equilibrium was attained. The mass of wet membrane (W_w) was measured after removing the surface water with blotting paper. SI was calculated on the basis of following formula:

$$SI(\%) = \left[\frac{(W_w - W_d)}{W_d}\right] \times 100\% \quad (4)$$

Ionic conductivity of HTCH membranes was calculated through impedance analysis [22] in which a Hewlett-Packard model 4194A impedance/gain-phase analyzer was employed. Complex impedance measurements were carried out in the AC mode, in the frequency range within 0.1–10^4 kHz, with a 0.1 V amplitude of AC signal. In the case of dry membranes, they were sandwiched between two brass blocking electrodes in the measurement cell for data collection. In the case of measurements for the hydrated membranes, dry membranes were immersed in deionized water at room temperature for 2 h prior to measurements, surface water was carefully removed, and the swollen membrane was quickly placed between electrodes in the measurement cell. The water content of membranes was assumed to remain constant during the short period of time required for measurements.

3. Results and discussion

3.1. Synthesis of HTCC

Fig. 1 presents IR spectra of chitosan and HTCC, respectively. In Fig. 1(A), a band at 1581 cm^{-1} can be attributed to amino groups of chitosan, and a shoulder at around 1660 cm^{-1} is usually recorded for chitosan with a high degree of deacetylation [22]. A strong band corresponding to the C–H bending of trimethylammonium group is registered at 1480 cm^{-1} in Fig. 1(B), confirming the existence of the quaternary ammonium salt [23]. It is also noted that the peak originally corresponding to the primary amine (1581 cm^{-1}) of chitosan disappears, and a new peak at around 1648 cm^{-1} for HTCC is observed, clearly revealing that the primary amine of chitosan backbone was already changed into a secondary amine structure due to the reactions associated with glycidyltrimethylammonium chloride (GTMAC).

Fig. 2 shows the ^{1}H NMR spectrum of HTCC. A very strong peak at around 3.2 ppm was observed, indicating the presence of methyl groups in the quaternary ammonium side chains. The remnant peaks, assigned respectively to protons in chitosan backbone and

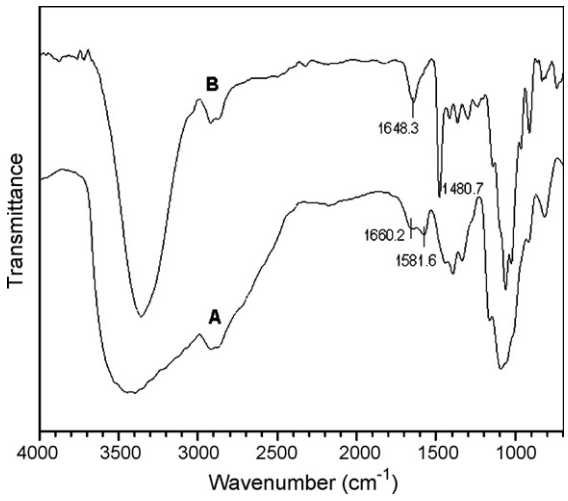

Fig. 1. FTIR spectra of (A) chitosan and (B) HTCC (DQ: 73.6%).

in quaternized side chains, were well in agreement with reported results [23,26]. On the basis of IR and ^{1}H NMR spectra of HTCC, it can be concluded that quaternary ammonium side chains have been successfully grafted on chitosan main chains. Based on many trials, it was attained that by changing GTMAC/chitosan feed ratios and selecting appropriate reaction temperature and time, DQ of HTCC could be well controlled. A series of HTCC samples was thus synthesized and the relevant parameters are summarized in Table 1. As mentioned in experimental section, DQs of HTCC were measured using either titration or elemental analysis. The data for DQs in Table 1 show basic consistency and thus confirm that present synthesis technique is stable and well controllable. In addition, it can be

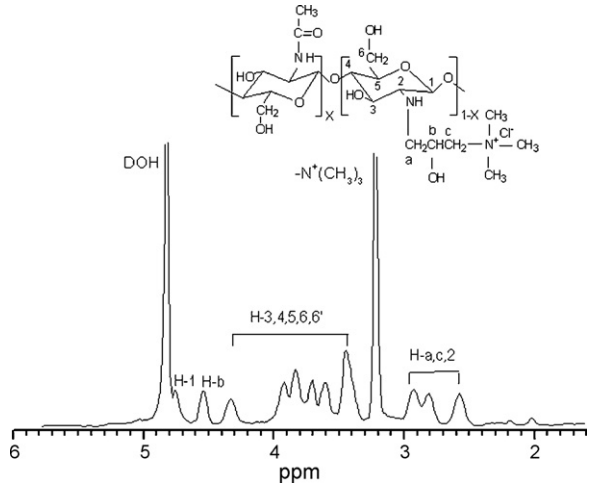

Fig. 2. ^{1}H NMR spectrum of HTCC (DQ: 78.3%).

Table 1
Parameters of HTCC[a].

Samples	Feed ratio of GTMAC to chitosan (m mol/m mol)	DQ (%)		Solubility in water[b]
		Titration	Elemental analysis	
HTCC (I)	42/30	21.5(±2.6)	22.2(±1.7)	±
HTCC (II)	63/30	34.8(±2.4)	33.3(±1.6)	±±
HTCC (III)	84/30	51.7(±2.7)	49.5(±1.8)	±±
HTCC (IV)	104/30	68.4(±2.9)	71.8(±2.1)	±±
HTCC (V)	125/30	83.6(±3.5)	81.9(±2.3)	+

[a] Data in table are calculated as averages from five specimens for each sample.
[b] +, soluble; ±± partially soluble or highly swelled; ±, swelled.

seen in Table 1 that although GTMAC/chitosan feed ratios were set to increase in an almost proportional manner, DQ of HTCC increased in an obviously nonlinear style, and the resultant HTCC exhibited various solubilities which were significantly dependent on DQ. Various solubilities for different HTCC also further demonstrate that quaternary ammonium side chains have been successfully grafted onto chitosan chains because unmodified chitosan is insoluble or not swelling in water.

3.2. Crosslinked HTCH membranes

Glutaraldehyde (GA) is a very common crosslinker used for crosslinking chitosan membranes. A typical mechanism suggested is Shiff-base formation between the amino groups of chitosan and the aldehyde groups of GA [27]. However, it has been found that GA is not an effective crosslinker for quaternized-chitosan having a relatively high DQ (for example, DQ > 35%) [21] because the resultant membranes could be highly swollen and show poor mechanical properties. It has been reported that ethylene glycol diglycidyl ether (EGDE) is able to crosslink chitosan molecules by anchoring two epoxy groups of EGDE respectively on two amino groups in different chitosan chains to form a real covalent linkage [28], and therefore, it is apparently worthy of exploring the possibility about crosslinking quaternized-chitosan membranes by using EGDE. In principle, there are different pathways to prepare crosslinked quaternized-chitosan membranes by using either HTCC or HTCH. In the case of HTCC, the resultant membranes have to be post-processed to remove chloride ions inside membranes because HTCC is a chloride-form quaternized-chitosan derivative and the membranes composed of HTCC cannot be used for alkaline fuel cells. HTCH can be exempt from post-processing since HTCH has already been a hydroxide-form quaternized-chitosan derivative. In spite of two available pathways, based on many trials, it was found that the HTCC membranes crosslinked by using EGDE were usually swollen and cracked during the post-processing in a basic solution, suggesting that directly crosslinking HTCC is unadvisable. To keep away from crosslinking HTCC, a specially designed processing technique has been developed in the present study. By reacting HTCC with a 1.0 M KOH solution for a given time to detach Cl^- ions and further removing residual KOH via a dialysis procedure, highly swollen HTCH gels have been obtained. By optimizing processing parameters, these gels can be successfully crosslinked with EGDE, and the structures and properties of resultant membranes can also be well controlled. Fig. 3 illustrates relevant details about reaction procedures and the final structure of crosslinked HTCH membranes.

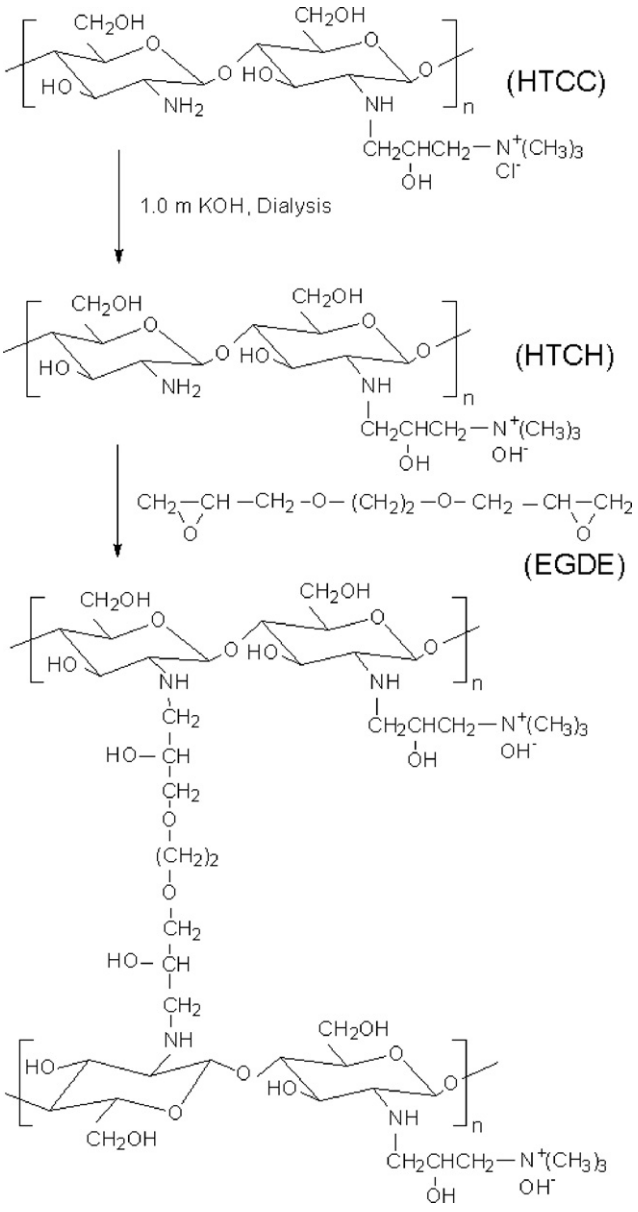

Fig. 3. The structure of crosslinked HTCH membranes.

Considering some amino groups in HTCH backbone should be saved for EGDE-involved crosslinking reactions and degree of deacetylation of starting chitosan powder is about 97%, DQs of HTCHs were therefore controlled not higher than 75% even though a higher DQ would possibly endow the crosslinked HTCH membrane a higher ionic conductivity. In addition, it was also found that under present reaction and processing conditions the crosslinked HTCH membranes would show poor mechanical properties when HTCHs with a DQ higher than 80% were selected. It the present study, all EGDE-crosslinked HTCH membranes were thus prepared using HTCHs with a DQ lower than 75% and the relevant parameters for these membranes are summarized in Tables 2 and 3. It is worth mentioning out that the feed ratio of EGDE to HTCH was set as 0.5/6.0 (m mol/m mol) for these membranes in Table 3 on the basis of many trials since the membranes with a DQ higher than ca. 55% could not be well crosslinked if the amount of crosslinker is lower than this selected value. In addition, the targeted mem-

Table 2
Parameters of crosslinked HTCH membranes with a constant DQ[a,b].

Samples	Feed ratio of EGDE to HTCH (m mol m mol^{-1})	ρ ($\times 10^{-2}$ mol g^{-1})	IEC (m eq. g^{-1})
HTCH-a	0.1/6.0	1.21(±0.11)	0.83(±0.05)
HTCH-b	0.2/6.0	1.32(±0.09)	0.81(±0.06)
HTCH-c	0.3/6.0	1.47(±0.12)	0.85(±0.05)
HTCH-d	0.4/6.0	1.64(±0.11)	0.82(±0.04)
HTCH-e	0.5/6.0	1.86(±0.07)	0.86(±0.05)
HTCH-f	0.6/6.0	2.08(±0.09)	0.82(±0.07)

[a] All membranes were prepared using a same kind of HTCH having a DQ was 70.4(±2.2) %, determined by the elemental analysis.
[b] The thickness of membranes was 110–130 μm in their dry state.

Table 3
Parameters of crosslinked HTCH membranes with various DQs[a].

Samples	DQ (%)[b]	ρ ($\times 10^{-2}$ mol g^{-1})	IEC (m eq. g^{-1})
HTCH-1	21.8(±1.9)	2.21(±0.09)	0.33(±0.04)
HTCH-2	30.2(±2.2)	2.13(±0.08)	0.41(±0.05)
HTCH-3	41.5(±1.8)	2.08(±0.11)	0.52(±0.06)
HTCH-4	52.7(±1.9)	1.96(±0.08)	0.64(±0.05)
HTCH-5	60.6(±2.2)	1.89(±0.09)	0.76(±0.04)
HTCH-6	71.3(±2.1)	1.81(±0.08)	0.86(±0.06)

The thickness of membranes was maintained as the same as that showed in footnote b under Table 2.

[a] All membranes were prepared using a same feed ratio of EGDE to HTCH (0.5/6.0 m mol/m mol).

[b] DQs of membranes were determined by the elemental analysis.

branes in this study are expected to have an ionic conductivity as high as possible and therefore, some HTCHs with a relatively high DQ should be selected and thus a relatively large amount of crosslinker is concomitantly required.

Table 2 indicates that by maintaining DQ of HTCHs as a constant, the crosslinking density of membranes exhibits a significant increase with the increasing feed ratio of EGDE to HTCH. This is an expected result because the epoxy groups of EGDE reacts directly with $-NH_2$ groups at C-2 sites of chitosan backbone under the present reaction condition and the increased amount of EGDE would generate increasing linkages between different chitosan chains. Data in Table 3 reveal that by keeping the amount of crosslinker unchanged, crosslinking density of membranes measurably decreases with increasing DQs. This trend possibly arises from following facts. HTCH with a higher DQ have two features: (1) a less amount of residual free amino groups on its backbone, and (2) a larger amount of quaternary side chains, compared to a HTCH having a lower DQ. The first feature of HTCH with a higher DQ would reduce reaction rate of EGDE with HTCH and the second feature could establish a more bulky environment and hinder $-NH_2$ groups on the backbone from reacting with epoxy groups of EGDE, endowing the resultant HTCH membranes an evidently lower crosslinking density. In addition, it is also observed that the series of HTCH-*i* ($i = a, \ldots, f$) membranes shows their changes in crosslinking density within an wider span compared to the series of HTCH-*j* ($j = 1, \ldots, 6$) membranes (see Tables 2 and 3), possibly implying that the amount of crosslinker would dominantly govern the crosslinking density of HTCH membranes.

3.3. Ion exchange capacity (IEC)

In principle, IEC of an ionic-conductive membrane usually reflects the amount of exchangeable groups in the membrane, and a relatively high IEC is normally correlative to a higher ionic conductivity [29]. IECs of all HTCH membranes were evaluated by titration and the collected data are provided in Tables 2 and 3. Data in Table 2 clarifies that there are no measurable differences observed among IECs of these membranes, suggesting that by fixing the DQ as constant, the amount of crosslinker would not substantially affect IECs of HTCH membranes. On the other hand, Table 3 verifies that by keeping the amount of crosslinker as constant, IECs of membranes significantly alter with DQ. As mentioned in experimental subsection, HTCH membranes were prepared with hydroxide-form quaternized-chitosan and therefore, IECs of membranes would mainly correspond to the amount of quaternary ammonium inside membranes even though the amino groups in chitosan backbone would also slightly contribute to these IECs. In the case of membranes listed in Table 2, since DQ is maintained unchanged and it is proportionally related to the amount of quaternary ammonium hydroxide, the result for those IECs are reasonable because crosslinking reactions only occurred at $R-NH_2$ and the unreacted amino groups would not substantially change IECs of membranes because of weak basic properties of amino groups compared to quaternary ammonium groups. Since the membranes presented in Table 3 were prepared by keeping the feed ratio of EGDE to HTCH unchanged and almost regularly altering DQ it is an expectant result that IECs of membranes increase with increasing DQ. By comparing the results in Table 3 with that in Table 2, and considering the effect of DQ and ρ on IECs, it can be reached that IECs of membranes would be mainly governed by the DQ of used HTCH.

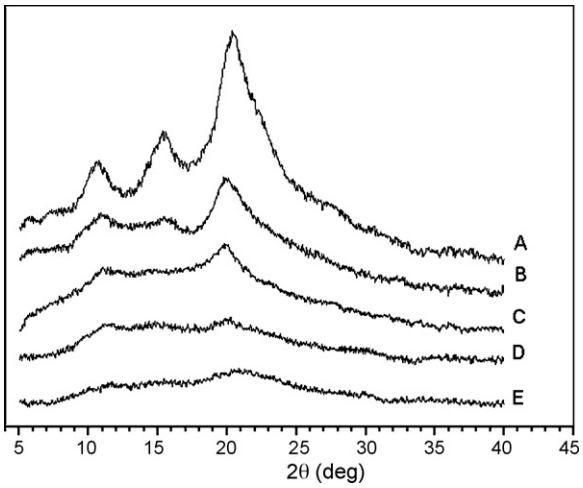

Fig. 4. X-ray diffraction patterns of different membranes. (A) Uncrosslinked chitosan membrane; (B) UN-HTCH (DQ: 21.8%); (C) UN-HTCH (DQ: 71.3%); (D) HTCH-1 and (E) HTCH-6.

3.4. Crystalline property of membranes

To make a comparison of crystalline properties among different membranes, some representative X-ray patterns are provided in Fig. 4. It is observed that the diffractogram of uncrosslinked chitosan membrane consists of three major crystalline peaks locating at around 10°, 15° and 20°, which are in well agreement with reported results [30]. The X-ray pattern of UN-HTCH (21.8%) that has a relatively low DQ exhibits some changes in both its diffraction angles and peak intensity compared to the uncrosslinked chitosan membrane. With respect to UN-HTCH (71.3%), having a much higher DQ compared to UN-HTCH (21.8%), the peak originally shown in the pattern of uncrosslinked chitosan membrane and concentrated at around 15° has completely disappeared, and two remnant peaks are shifted to ac.11° and 19° and remarkably weakened in their intensity compared to that of UN-HTCH (21.8%). These results reveal that the crystalline properties of UN-HTCH (*k*) membranes are significantly modulated by DQ. It is well known that the rigid structure of chitosan is mainly stabilized by the hydrogen bonds [31]. In the case of unmodified chitosan, the intramolecular hydrogen bonds are usually formed by amino groups at C-2 and hydroxyl groups at C-3 positions, and the intermolecular hydrogen bonds can be created between hydroxyl groups at C-6 and C-3 positions through absorbed water molecules. However, in the case of HTCH, the intermolecular and intramolecular hydrogen bonds would be drastically reduced because substituted quaternary side chains are much longer and bulkier than those original amino groups at the C-2 positions of chitosan, and would give a great degree of steric hindrance to formation of new hydrogen bonds. As a result, UN-HTCH (*k*) membranes are expected to show significantly decreased crystallinity compared to the uncrosslinked chitosan membrane, and this will specially true when the DQ is higher.

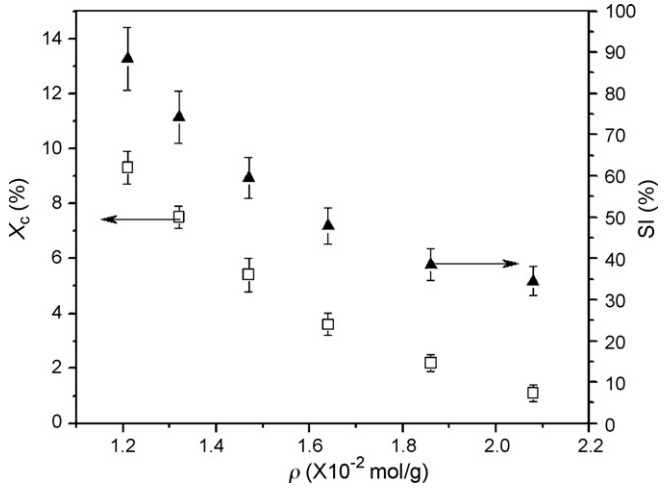

Fig. 5. The variance of crystallinity and SI of the membranes with crosslinking density (DQ: 71.3%).

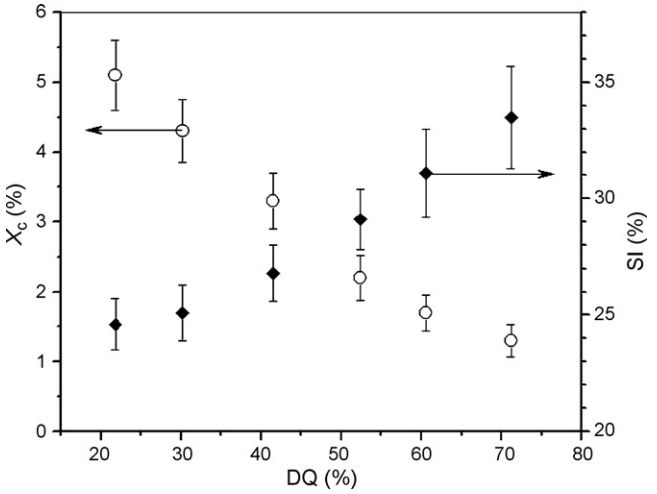

Fig. 6. The variance of crystallinity and SI of the membranes with degree of quaternization (feed ratio of EGDE to HTCH: 0.5/6.0 m mol/m mol).

UN-HTCH (21.8%) and HTCH-1 have the same DQ and the only difference between them is that the former is a uncrosslinked membrane and the latter has been crosslinked with EGDE. Fig. 4 shows that crystalline domains in HTCH-1 seem to be highly destroyed because only two very small peaks at around 11° and 19° have been noted. A similar behavior is also recorded for HTCH-6 that has a DQ matched with UN-HTCH (71.3%), and no evident peaks but some traces are observed in its X-ray pattern. These results may suggest that after being crosslinked, HTCH membranes tend to have an amorphous structure. Some data are provided in Figs. 5 and 6 to more detailed figure out the effect of DQ and ρ on the crystallinity of crosslinked HTCH membranes. Fig. 5 shows that crystallinity of HTCH-i ($i = a, \ldots, f$) membranes notably decreases with increased ρ; and Fig. 6 indicates that crystallinity of HTCH-j ($j = 1, \ldots, 6$) membranes progressively reduces as DQ increases. These results reveal that both ρ and DQ would modulate the crystalline properties of HTCH membranes, and ρ possibly plays a more important role since the crystallinity of membranes alters in a wider range in Fig. 5 than that in Fig. 6.

3.5. Water uptake

The swelling property of an ion exchange membrane will simultaneously affect dimensional stability of membranes and migration of ions inside [32]. In general, too high water uptake would possibly damage dimensional stability of membranes and also increase the resistance of membranes due to the increased thickness. However, the migration rate of ions inside membranes could be very low if water uptake is not sufficient enough. Therefore, water uptake sometimes needs to be carefully balanced. SI is a common parameter for estimating water uptake of membranes and the measured data for SI are depicted in Figs. 5 and 6 for following comparisons.

HTCHs with various DQs show quite different solubilities and some of them having a DQ higher than 70% are able to highly swollen or even dissolve in water (see Table 1). Fig. 5 indicates that SI of HTCH-i ($i = a, \ldots, f$) membranes dramatically drops down with increasing ρ, revealing water uptake of membranes can be efficaciously schemed by controlling the amount of crosslinker which is directly linked to ρ. It can be seen in Fig. 5 that some HTCH membranes are still quite swelling at lower ρ, as expressed by a high SI; and the SI of other HTCH membranes crosslinked with a higher amount of crosslinker (e.g. HTCH-d, HTCH-e and HTCH-f) seem to approximatively reach appropriate values [33]. Fig. 6 shows that by using the same amount of crosslinker, SI of membranes gradually increases with increasing DQ even though DQ imposes a much weaker impact on SI of membranes compared to ρ (see Figs. 5 and 6). In general, SI of a crosslinked chitosan membrane would be simultaneously modulated by the crystallinity and crosslinking density of the membrane [34]. However, in the present instance, effect of crystallinity on SI is very limited or even negligible since the crystalline domains of hydrated HTCH membranes would be damaged to a large extent or even completely destroyed, depending on the DQ of HTCHs because of increased hydrophilicity of HTCTs. Consequently, crosslinking density functions as a governing factor for SI of membranes. As indicated in Table 3, ρ decreased with increasing DQ when the same amount of crosslinker was employed, meaning that in the present cases, some hydrated membranes consisted of HTCHs with a higher DQ would have a lower ρ, which would certainly result in increased SI of membranes, as shown in Fig. 6.

3.6. Thermal stability

Durability of polymer electrolyte membranes is a very important factor in limiting the commercialization of polymer electrolyte membrane fuel cells [35–37]. Thermal stability of the membranes apparently plays a key role since these membranes have to function steadily and durably in different environments at various temperatures for a long term. Thermal degradation of some UN-HTCH (k) membranes and an uncrosslinked chitosan membrane was thus examined and several representative thermograms are represented in Fig. 7. To quantitatively find out the differences among these thermograms, the onset temperature of thermal degradation (T_{onset}, defined as a temperature corresponding to a weight loss of 5 wt%) is selected as a variable for the comparison. Fig. 7 displays that all UN-HTCH (k:DQ, k = 71.3%, 52.7% and 30.2%) membranes have a much lower T_{onset} compared to that of the uncrosslinked chitosan membrane, and meanwhile, T_{onset}s of the UN-HTCH (k) membranes pronouncedly decrease with increasing DQ. Possible reasons for UN-HTCH (k) membranes may arise from following facts. It is known that chitosan is a semi-crystalline polymer and grafting quaternary side chains onto chitosan backbone would definitely suppress the recrystallized ability of main chains and result in remarkably decreased crystallinity in UN-HTCH (k) membranes. In fact, Fig. 4 has demonstrated that UN-HTCH (21.8%) has a significantly lower crystallinity than that of uncrosslinked chitosan membrane, and UN-HTCH (71.3%) shows a more lower crystallinity compare to UN-HTCH (21.8%). Since the rigid crystalline structure of chitosan is mainly stabilized by hydrogen bonds [31] the

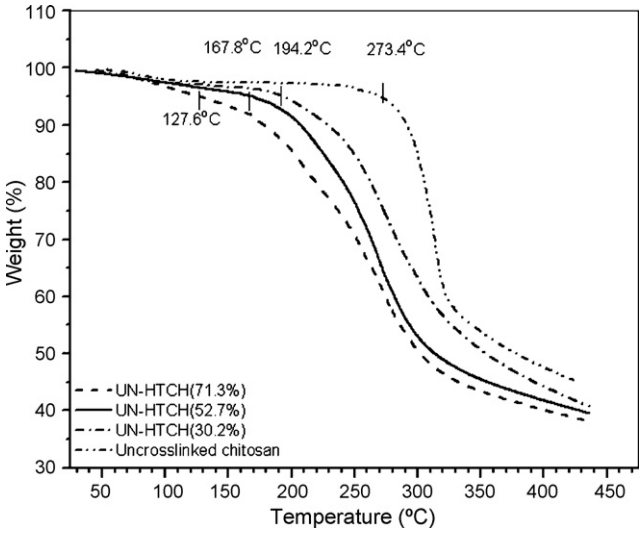

Fig. 7. TG thermograms of UN-HTCH (71.3%), UN-HTCH (52.7%), UN-HTCH (30.2%) and the uncrosslinked chitosan membrane.

decrease in crystallinity of an UN-HTCH (k) membrane, therefore, should mean a loss of interactions arising from hydrogen bonds. It is generally accepted that the intermolecular and intramolecular hydrogen bonds can contribute to maintaining thermal and mechanical stability of chitosan membranes [38], and thus it is an expectable result that the UN-HTCH (71.3%) membrane shows a lowest T_{onset} compared to UN-HTC H (52.7%), UN-HTCH (30.2%) and the uncrosslinked chitosan membrane because UN-HTCH (71.3%) has a highest DQ among them.

The thermograms of several HTCH-j (j = 2, 4 and 6) membranes are provided in Fig. 8. Since DQs of UN-HTCH (71.3%), UN-HTCH (52.7%) and UN-HTCH (30.2%) in Fig. 7 are exactly corresponded to the DQs of HTCH-6, HTCH-4 and HTCH-2 (see Table 3), respectively, only one difference exists between Figs. 7 and 8, namely, the series of UN-HTCH (k) (k = 71.3%, 52.7% and 30.2%) was not crosslinked but HTCH-6, HTCH-4 and HTCH-2 membranes were already crosslinked by EGDE. It can be easily seen that the HTCH-6 membrane shows its T_{onset} as high as ca. 194 °C which is around 67 °C higher than that of UN-HTCH (71.3%), and HTCH-4 and HTCH-2 also exhibit significantly increased T_{onset} compared with UN-HTCH (52.7%) and

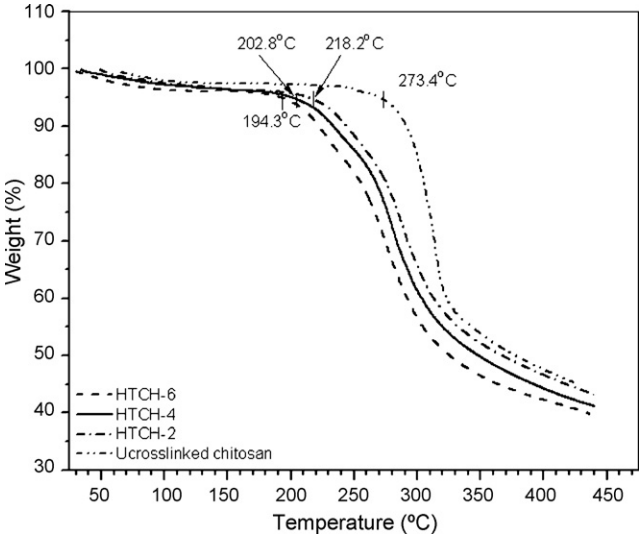

Fig. 8. TG thermograms of HTCH membranes and the uncrosslinked chitosan membrane (feed ratio of EGDE to HTCH: 0.5/6.0 m mol/m mol).

Table 4
Thermal stability of crosslinked HTCH membranes.

Samples[a]	T_{onset} (°C)	Samples[b]	T_{onset} (°C)
HTCH-a	157.3(±2.3)	HTCH-1	235.4(±0.6)
HTCH-b	169.7(±2.1)	HTCH-2	219.7(±0.7)
HTCH-c	180.2(±1.7)	HTCH-3	211.6(±0.8)
HTCH-d	196.5(±1.6)	HTCH-4	203.9(±0.7)
HTCH-e	209.6(±1.2)	HTCH-5	199.2(±0.9)
HTCH-f	221.8(±0.9)	HTCH-6	195.7(±1.1)

[a] See Table 2 for parameters of membranes.
[b] See Table 3 for parameters of membranes.

UN-HTCH (30.2%), respectively, revealing that thermal stability of the crosslinked HTCH membranes has been considerably improved.

All crosslinked HTCH membranes were measured for their T_{onset} and collected data are listed in Table 4. As indicated in Table 2, the set of HTCH-i(i = a, . . ., f) membranes was prepared using the same HTCH but with various amounts of EGDE, the data in Table 4 manifest that T_{onset} of the HTCH-i (i = a, . . ., f) membranes notably increases with the increasing amount of EGDE, and also with increasing ρ. The series of HTCH-j (j = 1, . . ., 6) membranes was produced with different HTCHs but using a fixed amount of EGDE (see Table 3), and their T_{onset}s are shifted to lower temperatures as DQ of HTCHs increases. These results suggest that thermal stability of the crosslinked HTCH membranes would be regulated by both ρ and DQ of the membranes but more dominantly by ρ.

Although T_{onset} of all crosslinked HTCH membranes showed in Table 4 are still much lower than that of uncrosslinked chitosan membrane, these membranes are considered to be thermally stable enough for practical applications because they will be possibly used only in low-temperature alkaline fuel cells where the operation temperature is usually lower than 100 °C.

3.7. Ionic conductivity

Several crosslinked membranes after being hydrated for 2 h at room temperature, were measured for their ionic conductivity using impedance spectroscopy and the resultant plots of imaginary impedance ($-Z''$) versus real impedance (Z') are presented in Fig. 9. These spectra consist of two typical regions in the complex plane: a partial semicircle arc in the high frequency zone and a linear region in the low-frequency zone [39]. HTCH-b and HTCH-e membranes show similar ionic-conductive behaviors with a small difference in the intercepts of the complex impedance plots at the real axis (Z' axis). On the other hand, a large difference in the impedance spec-

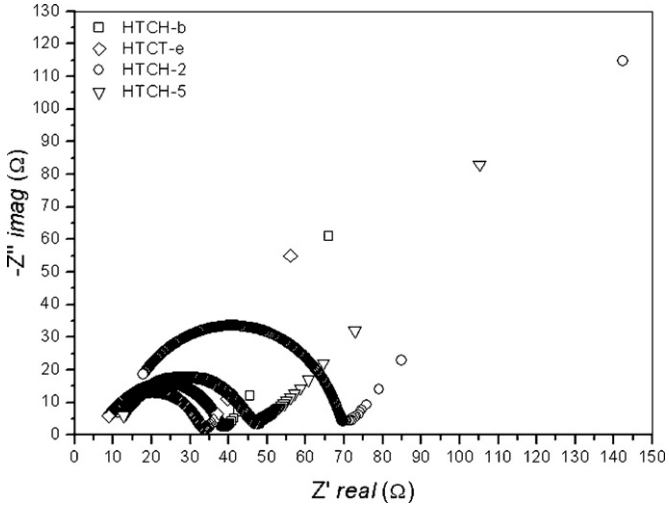

Fig. 9. Impedance spectra of HTCH membranes after hydration.

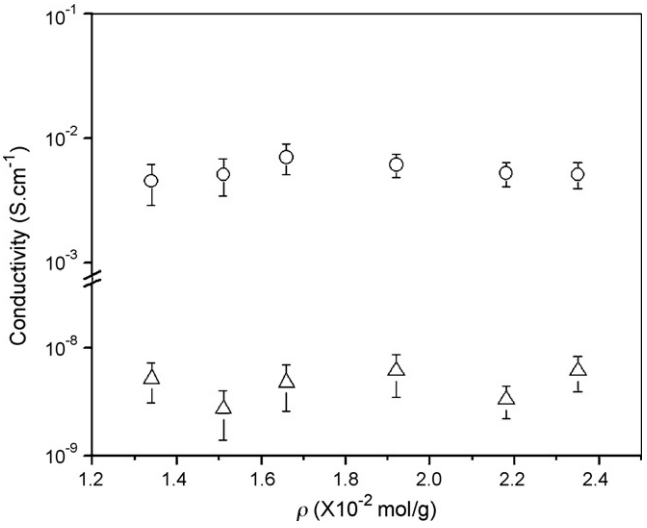

Fig. 10. Ionic conductivity of membranes with varied crosslinking densities before (△) and after (○) hydration (DQ: 70.4 (±2.2) %).

tra of HTCH-2 and HTCH-5 membranes is registered, and HTCH-5 membrane exhibits a notably higher ionic conductivity compared to HTCH-2.

To make more detailed comparisons, all membranes were subjected to impedance measurements before and after hydration, and the collected data are depicted in Figs. 10 and 11, respectively. It can be observed that all HTCH membranes in their dry state only exhibited ionic conductivities close to 10^{-8} S cm^{-1}, and the conduction process occurred after the membranes were fully hydrated. Fig. 10 indicates that although average values of conductivity seem to slightly change there is not a substantial difference in the conductivity recorded for these membranes if standard deviations are included for the comparisons. On the other hand, the data displayed in Fig. 11 reveal that conductivity significantly increases with incremental DQ. These results may reveal that conductivity of membranes would be chiefly modulated by DQ of the membranes even though the conduction process of membranes could also be somewhat influenced by water uptake [33]. In general, an increase in the water content in an ionic-conductive membrane may facilitate the migration of ions, which would enhance the conductivity of the membrane. However, the increased amount of water uptake will certainly dilute ion concentration and further extend the distance of ion-migration due to the swelling of the membrane, which will in turn give rise to additional resistance in the path of ion-migration. Consequently, effect of water uptake could be counteracted due to pros and cons of impacts and the conductivity of membrane is mainly governed by the concentration of free ions, which is actually correlated with IEC of membranes [29]. In fact, the conductivity of membranes vs. DQ is quite equivalent to the conductivity vs. IEC of membranes because DQ and IEC behaved a similar trend (see Table 3). Above results may suggest that some HTCHs with a higher DQ should be preferentially selected to endow the crosslinked HTCH membranes higher conductivity whereas the crosslinking density, which is indirectly correlated to water uptake (see Figs. 7 and 8), is acting as a subordinate factor for the conductivity of membranes.

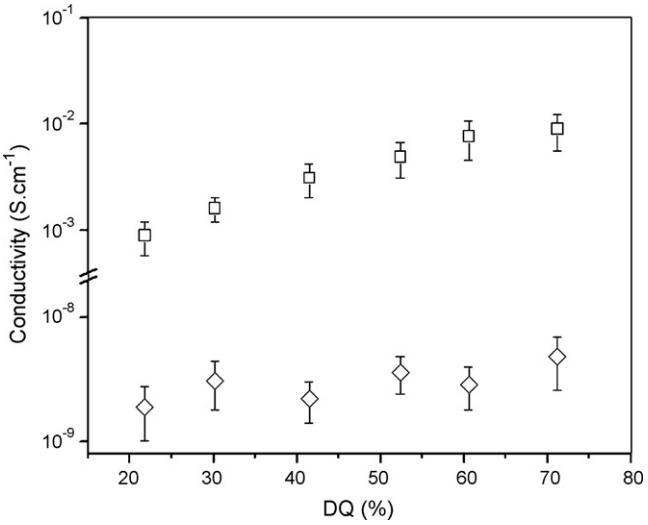

Fig. 11. Ionic conductivity of membranes with varied degrees of quaternization before (◊) and after (□) hydration (feed ratio of EGDE to HTCH:0.5/6.0 m mol/m mol^{-1}).

Nafion® N117 is a commonly available membrane used in practical fuel cell systems and shows ionic conductivity of around 0.08 S cm^{-1} and IEC of about 0.91 (m eq. g^{-1}) [40,41]. Some crosslinked HTCH membranes (for example, HTCH-d, HTCH-e, HTCH-f, HTCH-5 and HTCH-6) obtained in this work exhibit good physical properties and their ionic conductivity and IEC are close to that of N117 membranes although it is important to point out that there is a fundamental difference in that the N117 membrane is a proton conductor and the HTCH membrane is a hydroxide conductor. In considering all results together, it could be concluded that some HTCH membranes are promising candidates for alkaline polymer electrolyte fuel cells. Following investigations for their mechanical properties and applications in alkaline fuel cells are being conducted and relevant results will be given in separate reports.

4. Conclusions

A number of quaternized-chitosan derivatives with various degrees of quaternization up to 70% were first synthesized, and they were further successfully prepared into crosslinked membranes via a newly developed processing technique. These crosslinked quaternized-chitosan membranes showed controllable characteristics and the main properties such as crystallinity, swelling index, ion exchange capacity, ionic conductivity and thermal stability could be effectively regulated by both degree of quaternization and crosslinking density of membranes. Of these two overriding factors, crosslinking density played a more important role to modulate the crystallinity, swelling index and thermal stability of membranes. It was observed that the thermal stability of membranes was enhanced with increasing crosslinking density but both crystallinity and swelling index of membranes decreased as crosslinking density was increased. It was also found that the ion exchange capacity and ionic conductivity of membranes were dominantly governed by the degree of quaternization of membranes, and they both significantly increases with increasing degree of quaternization. Some crosslinked quaternized-chitosan membranes exhibited good integrated properties and had potential for applications in alkaline polymer electrolyte fuel cells.

Acknowledgement

The financial support for this work was provided by the Natural Sciences and Engineering Research Council of Canada.

References

[1] J.R. Varcoe, R.C.T. Slade, Fuel cells 5 (2005) 187.
[2] O. Savadogo, J. New Mater. Electrochem. Syst. 1 (1998) 47.
[3] G.F. McLean, T. Niet, S. Prince-Richard, N. Djilali, Int. J. Hydrogen Energy 27 (2002) 507.

[4] C. Lamy, E.M. Belgsir, J.M. Leger, J. Appl. Electrochem. 31 (2001) 799.
[5] E.H. Yu, K. Scott, R.W. Reeve, J. Electroanal. Chem. 547 (2003) 17.
[6] S. Gamburzev, K. Petrov, A.J. Appleby, J. Appl. Electrochem. 32 (2002) 805.
[7] K. Scott, P. Argyropoulos, P. Yiannopoulos, W.M. Taama, J. Appl. Electrochem. 31 (2001) 823.
[8] D.P. Davies, P.L. Adcock, M. Turpin, S.J. Rowen, J. Appl. Electrochem. 30 (2000) 101.
[9] B. Krajewska, J. Chem. Technol. Biotechnol. 76 (2001) 636.
[10] Y. Wan, K.A.M. Creber, B. Peppley, V.T. Bui, J. Appl. Polym. Sci. 89 (2003) 306.
[11] Y. Wan, K.A.M. Creber, B. Peppley, V.T. Bui, E. Halliop, J. Power Sources 162 (2006) 105.
[12] T.N. Danks, R.C.T. Slade, J.R. Varcoe, J. Mater. Chem. 13 (2003) 712.
[13] G. Wang, Y. Weng, D. Chu, D. Xie, R. Chen, J. Membr. Sci. 326 (2009) 4.
[14] Y. Xiong, Q.L. Liu, A.M. Zhu, S.M. Huang, Q.H. Zeng, J. Power Sources 186 (2009) 328.
[15] Y. Xiong, J. Fang, Q.H. Zeng, Q.L. Liu, J. Membr. Sci. 311 (2008) 319.
[16] C.C. Yang, S.J. Lin, G.M. Wu, Mater. Chem. Phys. 92 (2005) 251.
[17] C.C. Yang, S.J. Chiu, W.C. Chien, J. Power Sources 162 (2006) 21.
[18] C.H. Kim, J.W. Choi, H.J. Chung, K.S. Choi, Polym. Bull. 38 (1997) 387.
[19] Z. Jia, D. Shen, W. Xu, Carbohydr. Res. 333 (2001) 1.
[20] Y. Xiong, Q.L. Liu, Q.G. Zhang, A.M. Zhu, J. Power Sources 183 (2008) 447.
[21] Y. Wan, K.A.M. Creber, B. Peppley, V.T. Bui, E. Halliop, J. Power Sources 185 (2008) 183.
[22] Y. Wan, K.A.M. Creber, B. Peppley, V.T. Bui, Polymer 44 (2003) 1057.
[23] S.H. Lim, S.M. Hudson, Carbohydr. Res. 339 (2004) 313.
[24] J. Wu, Z.G. Su, G.H. Ma, Int. J. Pharm. 315 (2006) 1.
[25] T. Uragami, T. Katayama, T. Miyata, H. Tamura, T. Shiraiwa, A. Higuchi, Biomacromolecules 5 (2004) 1567.
[26] H.S. Seong, H.S. Whang, S.W. Ko, J. Appl. Polym. Sci. 76 (2000) 2009.
[27] G.A.F. Roberts, K.E. Taylor, Makromol. Chem. 190 (1989) 951.
[28] T. Uragami, M. Takuno, T. Miyata, Macromol. Chem. Phys. 203 (2002) 1162.
[29] J. Larminie, A. Dicks, Fuel Cell System Explained, 2nd ed., John Wiley and Sons, Chichester, UK, 2003.
[30] R.J.J. Samuels, J. Polym. Sci., Polym. Phys. Ed. 19 (1981) 1081.
[31] S.I. Nishimura, O. Kohgo, K. Kurita, H. Kuzuhara, Macromolecules 24 (1991) 4745.
[32] J.A. Kerres, Fuel Cells 5 (2005) 230.
[33] T.A. Zawodzinski, C. Derouin, S. Radzinski, R.J. Sherman, V.T. Smith, T.E. Springer, S. Gottesfeld, J. Electrochem. Soc. 140 (1993) 1041.
[34] Y. Yu, W. Li, T. Yu, Polym. Commun. 31 (1990) 319.
[35] J. Wu, X.Z. Yuan, J.J. Martin, H. Wang, J. Zhang, J. Shen, S. Wu, W. Merida, J. Power Sources 184 (2008) 104.
[36] R.L. Borup, J.R. Davey, F.H. Garzon, D.L. Wood, M.A. Inbody, J. Power Sources 163 (2006) 76.
[37] W. Schmittinger, A. Vahidi, J. Power Sources 180 (2008) 1.
[38] R.H. Chen, J.H. Lin, M.H. Yang, Carbohydr. Polym. 31 (1996) 141.
[39] P.D. Beattie, F.P. Orfino, V.I. Basura, K. Zychowska, J. Ding, C. Chuy, J. Schmeisser, S. Holdcroft, J. Electroanal. Chem. 503 (2001) 45.
[40] S. Gottesfeld, T.A. Zawodzinski, Electrochem. Sci. Eng. 5 (1997) 195.
[41] J.J. Sumner, S.E. Creager, J.J. Ma, D.D. DesMarteau, J. Electrochem. Soc. 145 (1998) 107.